Infection and Drug Resistance

Dovepress
Taylor & Francis Group

Open Access Full Text Article

ORIGINAL RESEARCH

Fluconazole-Decorated Gold Nanoparticles as a Novel Therapeutic Strategy Against Carbapenem-Resistant *Klebsiella pneumoniae*

Yuhan Yang[1,2], Juan Pan[1], Zeyong Zhong[2], Yanchun Gong[1], Zhuocheng Yao[1], Tieli Zhou[1], Jianming Cao[2], Chunquan Xu[1]

[1]Department of Clinical Laboratory, The First Affiliated Hospital of Wenzhou Medical University, Key Laboratory of Clinical Laboratory Diagnosis and Translational Research of Zhejiang Province, Wenzhou, Zhejiang, People's Republic of China; [2]School of Laboratory Medicine and Life Science, Wenzhou Medical University, Wenzhou, Zhejiang, People's Republic of China

Correspondence: Jianming Cao, School of Laboratory Medicine and Life Science, Wenzhou Medical University, Wenzhou, Zhejiang, People's Republic of China, Email wzcjming@163.com; Chunquan Xu, Department of Clinical Laboratory, The First Affiliated Hospital of Wenzhou Medical University, Key Laboratory of Clinical Laboratory Diagnosis and Translational Research of Zhejiang Province, Wenzhou, Zhejiang, People's Republic of China, Email 417242374@qq.com

Purpose: The alarming rise of carbapenem-resistant *Klebsiella pneumoniae* (CRKP) has escalated into a formidable global health threat, because of its steadily increasing resistance rates to therapeutically important antimicrobial treatments. To address this challenge, we synthesized fluconazole-decorated gold nanoparticles (FCZ_Au NPs) and evaluated the antibacterial efficacy.

Methods: FCZ_Au NPs were synthesized using a one-pot method. Its antimicrobial activity, anti-biofilm activity and antimicrobial mechanisms through antimicrobial susceptibility testing, growth curve analysis, murine model of acute intraperitoneal infection, crystal violet staining, reactive oxygen species (ROS) detection, membrane permeability assay.

Results: As determined by our assays, the minimum inhibitory concentration of FCZ_Au NPs against CRKP was found to be between 4 and 16 μg/mL, indicating strong inhibitory effects on bacterial growth. Furthermore, at the experimental concentrations, FCZ_Au NPs exhibited excellent safety profiles toward red blood cells and mouse RAW264.7 cells. In an acute intra-abdominal infection paradigm, a notable rise in the mice's survival rate and a commensurate decrease in the bacterial burden in peritoneal lavage fluid revealed the in vivo efficiency of FCZ_Au NPs. Investigations into the antibacterial mechanisms revealed that FCZ_Au NPs act by disrupting bacterial cell membranes and enhancing reactive oxygen species production. The crystal violet assay revealed the great potential of FCZ_Au NPs in inhibiting biofilm formation and eradicating mature biofilms.

Conclusion: In this study, we utilized the clinically antifungal drug FCZ to modify gold nanoparticles, synthesizing FCZ_Au NPs. Beyond their significant antibacterial activity against CRKP, these nanoparticles also demonstrated a strong ability to combat biofilms. Thus, this study provides a novel strategy for combating CRKP.

Keywords: carbapenem-resistant *Klebsiella pneumoniae*, fluconazole, gold nanoparticles, antibacterial activity

Introduction

The escalating crisis of antimicrobial resistance is profoundly exacerbated by opportunistic pathogens such as *Klebsiella pneumoniae*, an organism distinguished by its alarming capacity to cause a diverse spectrum of systemic infections.[1] These range from pneumonia and urinary tract infections to bacteremia and invasive liver abscesses, underscoring its clinical versatility and the urgency of the threat it poses.[2] Due to its extensive resistance to most clinical antimicrobial agents, *K. pneumoniae* has become a major contributor to the antibiotic resistance crisis. Figure 1 illustrates the common mechanisms by which bacteria develop drug resistance. This pathogen is estimated to cause more than over one hundred thousand deaths annually.[3] The World Health Organization (WHO) has designated Carbapenem-resistant *K. pneumoniae* (CRKP) as a critical-priority pathogen, a status driven by the escalating global challenge of healthcare-associated infections caused by multidrug-resistant, extended-spectrum β-lactamases, and carbapenemase-producing strains. Over

https://doi.org/10.2147/IDR.S588073
Received: 30 December 2025
Accepted: 10 March 2026
Published: 19 April 2026

Graphical Abstract

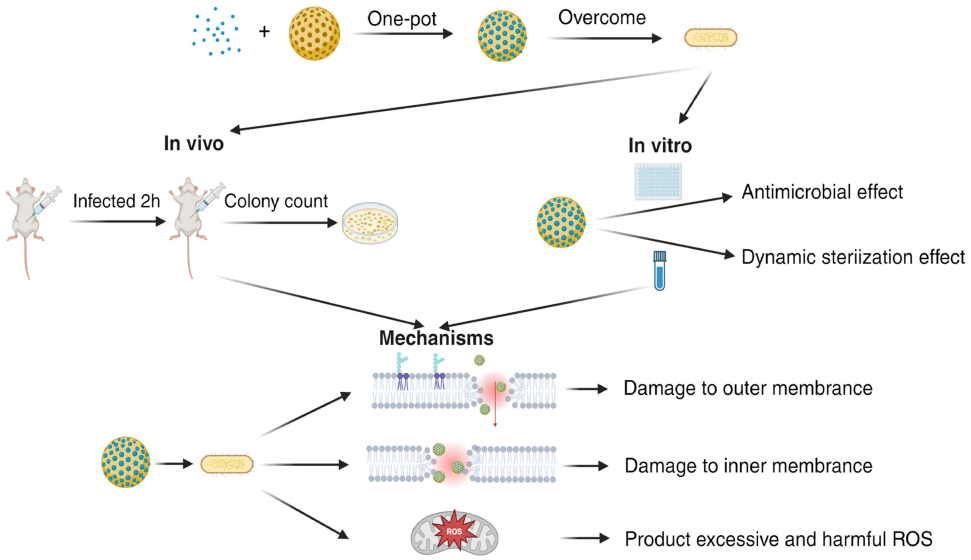

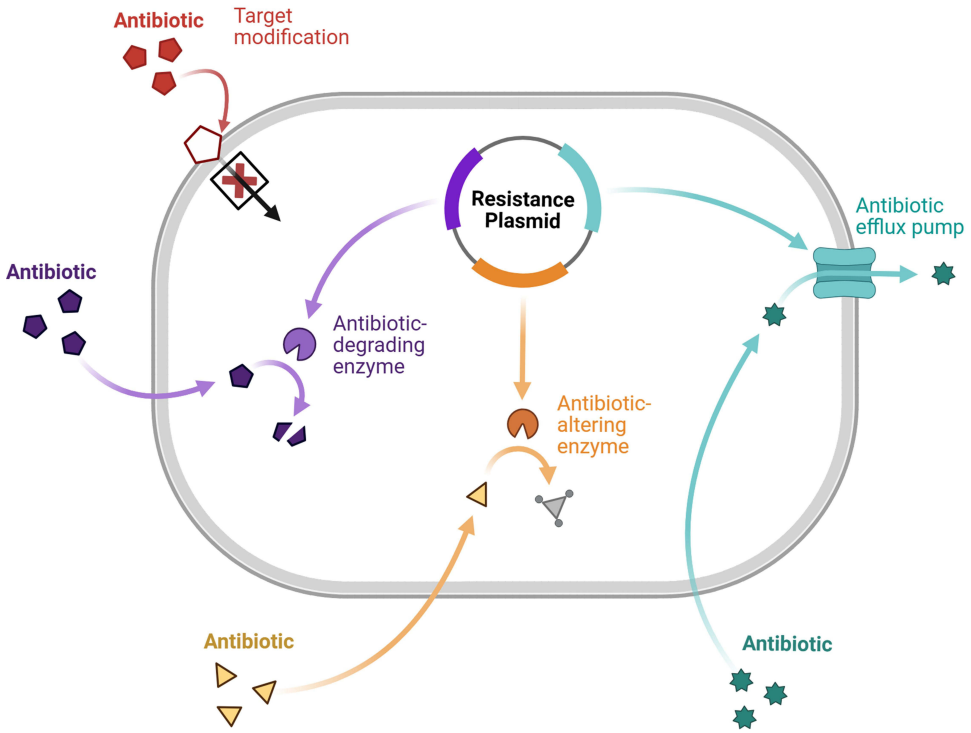

Figure 1 Diagrammatic representation of bacterial resistance mechanisms.

the past decade, these infections have solidified into a grave and persistent challenge for both clinical management and public health infrastructure worldwide.[4–6]

To tackle CRKP, new antimicrobial medicines are desperately needed. The development of novel therapeutic strategies targeting CRKP faces challenges such as lengthy cycles, high costs, and low success rates, highlighting the urgent need for alternative strategies such as drug repurposing or structural modification of existing compounds. In

addition to these obstacles, current clinical strategies for managing CRKP infections each has limitations: Although combination regimens represented by ceftazidime-avibactam have been clinically applied, and literature reports that combinations such as tigecycline with rifampicin enhance antibacterial activity against CRKP, such therapies still face inherent limitations. While combination therapy can enhance efficacy in the short term, it is often constrained by issues such as differences in drug solubility and cross-resistance; Furthermore, studies have shown that various antimicrobial peptides, including Cecropin-4 and Osmin, exhibit antibacterial activity against CRKP. However, antimicrobial peptides are difficult to widely apply due to their susceptibility to protease degradation and poor in vivo stability; Phage therapy, meanwhile, has relatively limited practical use because of its highly specific host targeting and tendency to trigger bacterial immune evasion.[7–13] These limitations compel researchers to explore antimicrobial approaches with entirely new mechanisms of action.

Nanotechnology, which involves creating materials with dimensions of 1–100 nm, is advancing at a remarkable pace.[14] The small size enable their effective dispersion within tissues.[15] They often exhibit unique physicochemical properties, along with biological activities such as antibacterial and antiviral effects,[16] demonstrating significant application potential. This technology has been widely applied in areas such as environmental protection, health, medicine, agriculture, and food science.[17] Among various nanomaterials, gold and silver nanoparticles have been extensively investigated for biomedical applications.[18] A prominent research focus lies in their green synthesis, which capitalizes on biological sources such as plants and microorganisms for production.[19–23] According to existing literature, silver and gold nanoparticles synthesized via green methods using fruit waste exhibit significant antibacterial activity against foodborne pathogens.[24] Moreover, green-synthesized gold nanoparticles not only demonstrate antibacterial effects but also show notable anti-biofilm activity.[25,26] Previous studies have reported that nanomaterials are capable of combating acquired antibiotic resistance and biofilm-associated bacterial infections.[27] However, existing research on nanoparticles for the treatment of CRKP has several limitations: insufficient characterization of bacterial resistance mechanisms, inadequate evaluation of biocompatibility, and a systematic evaluation of the antimicrobial potential of drug-functionalized gold nanoparticles remains limited.

Fluconazole (FCZ), a triazole antifungal agent, inhibits fungal cell membrane synthesis and is primarily used to treat *Candida albicans* infections.[28–30] However, its relatively large molecular size, hydrophobicity, and low solubility pose significant challenges for topical application. To address these limitations, researchers have loaded FCZ onto nanomaterial surfaces to enhance drug delivery and improve skin penetration.[31] The antifungal drug FCZ has a well-established safety profile in clinical applications. According to previous studies, the co-release of nitric oxide and FCZ from the same biomaterial surface can effectively combat both *Candida albicans* and *Escherichia coli*.[32] The triazole ring is a molecular structure within fluconazole. The nitrogen atoms in the triazole ring contain lone pair electrons, which exhibit high affinity for the surface of gold nanoparticles, enabling stable and firm binding to form a stable nanoconjugate. The fluconazole molecule possesses certain amphiphilic properties, and its structure may help nanoparticles anchor to or disrupt the bacterial cell membrane.[33,34] Therefore, immobilizing FCZ on biomaterial surfaces may not only improve its delivery efficiency but also potentially enhance its antimicrobial efficacy. Nevertheless, the application of FCZ-decorated gold nanoparticles (FCZ_Au NPs) for combating CRKP has not yet been explored. In this study, FCZ was conjugated to gold nanoparticle surfaces via a one-pot synthesis method, and the antibacterial efficacy of the resulting conjugate against CRKP was evaluated. This work provides a comprehensive evaluation of the anti-CRKP efficacy of FCZ_Au NPs. Furthermore, we elucidated the underlying antibacterial mechanisms, revealing the multifaceted nature of their action. We anticipate that this work will provide valuable mechanistic insights and present a viable nanotherapeutic strategy, thereby contributing to the future development of antimicrobial agents against CRKP.

Materials and Methods

Bacteria

The bacterial used in this study were eight clinical CRKP isolates and the quality control strain *K. pneumoniae* ATCC 700603. All clinical isolates were sourced from the First Affiliated Hospital of Wenzhou Medical University, with species identification confirmed by Matrix-Assisted Laser Desorption/Ionization Time-of-Flight Mass Spectrometry (MALDI-

TOF/MS; bioMérieux, Lyon, France). The clinically isolated strains used in this experiment were part of the routine hospital laboratory procedure. Prior to each experiment, strains were subcultured from these frozen stocks.

Preparation of FCZ_Au NPs and Au NPs

Gold nanoparticles (Au NPs) and FCZ_Au NPs were created using a one-pot green synthesis process based on previously published techniques.[35,36] Briefly, FCZ (0.05 mmol), Tween 80 (30 mg), and triethylamine (50 μL) were dissolved in 10 mL of double-distilled water (ddH_2O). Subsequently, the solution was stirred at 45°C and 500 μL of $HAuCl_4$ (0.05 mmol) was introduced for a 1.5 h under continuous stirring. The distinctive violet-black color of FCZ_Au NPs demonstrated the effective synthesis and confirmed through comprehensive characterization. In addition, the Au NPs without any decoration were synthesized via a sodium borohydride reduction method. Undecorated Au NPs were produced in an ice-water bath by swirling Tween 80 (30 mg) and $HAuCl_4$ (500 μL, 0.05 mmol) in 10 mL of cold water. An ice-cold aqueous solution of NaBH4 was then added dropwise, which immediately turned the solution brown. Stirring was continued for 1 h. Nanoparticles were dialyzed against ddH_2O for 24 h before being filtered through a 0.22 μm membrane for sterilization.

Characterization of FCZ_Au NPs

The ultraviolet-visible (UV-Vis) absorption spectrum was acquired with a BioTek Synergy NE02 microplate reader (USA). The hydrodynamic diameter and zeta potential were determined by dynamic light scattering (DLS; Malvern Zetasizer Pro, UK), while the nanoparticle morphology was visualized by transmission electron microscopy (TEM; FEI Talos F200S, USA). Furthermore, the surface chemistry was probed using Fourier-transform infrared spectroscopy (FTIR; Thermo Fisher Scientific Nicolet 6700, USA).

Antimicrobial Susceptibility Testing

We determined the minimum inhibitory concentration (MIC) by the microbroth dilution method in accordance with CLSI (M100, 35th ed., 2025) and EUCAST guidelines.[37] Briefly, antimicrobial agents, prepared at 4 times the final test concentration, were added to the last column and serially diluted two-fold across the plate. Subsequently, added 100 μL bacterial suspension. The plate was then incubated at 37°C. After 16–18 h, the MIC was defined as the lowest concentration of the agent that completely inhibited visible bacterial growth.

Growth Curve

The dynamic antimicrobial efficiency of FCZ_Au NPs was evaluated using a growth curve assay.[38] Briefly, the experiment included four groups: Phosphate-Buffered Saline (PBS), FCZ group, Au NPs group, and FCZ_Au NPs group. All agents were standardized to concentrations based on the MIC of FCZ_Au NPs, mixed with a bacterial suspension (1.5×10^6 CFU/mL), and incubated at 37°C. A full-wavelength microplate reader (Shandong Jingdao Optoelectronic Technology Co., Ltd. JD-QMBY, China) was used to measure the optical density at 600 nm at 0, 2, 4, 6, 12, and 24 hours.

Crystal Violet Staining Assay

The experiment included four groups, as described previously.[39] 100 μL of bacterial suspension mixed with 100 μL of the corresponding agents, the concentration of agents comparable to 0.5 × MIC of FCZ_Au NPs. After 24 h, the supernatant was discarded. The adhered biofilms were then gently rinsed and air-dried. Subsequently, the biofilms were stained by adding 0.1% crystal violet solution for 15 min, then rinsed off excess dye and air-dried again. The bound dye was eluted with 200 μL of a destaining solution (95% ethanol and 5% acetic acid), and the absorbance was measured at 595 nm.

The effectiveness of FCZ_Au NPs in eradicating preformed mature biofilms was assessed using a similar four-group. Mature biofilms were established by inoculating a bacterial suspension of 1.5×10^6 CFU/mL in LB broth and cultures at 37°C for 24 h. After careful remove the supernatant, 200 μL agents were added. Each at a concentration equal to the MIC of FCZ_Au NPs for the corresponding strain. Subsequent washing, staining, and elution steps were identical to the aforementioned procedure.

Reactive Oxygen Species Detection (ROS)

ROS levels were measured using the fluorescent probe 2',7'-dichlorodihydrofluorescein diacetate (DCFH-DA), in accordance with previously described methods.[40] Bacterial suspensions were loaded with 10 μmol/L DCFH-DA and incubated. Then centrifugated and washed three times to thoroughly remove unincorporated probe. Subsequently, the stained bacterial pellets were resuspended and treated with the respective agents for a specified duration. Finally, the fluorescence intensity was measured at excitation/emission wavelengths of 488/525 nm using a microplate reader.

Quantitative Real-Time PCR

Total RNA from each bacterial strain was extracted using the Trizol method.[41] Briefly, Trizol reagent, containing phenol and guanidine thiocyanate, was added to bacterial cells to lyse them and inhibit RNase activity. To separate the phases, the homogenate was mixed with chloroform, agitated briskly, then centrifuged. For precipitation, the RNA-containing aqueous phase was moved and combined with an equivalent amount of isopropanol. Following centrifugation and incubation, the RNA pellet was rinsed with 75% ethanol, allowed to air dry, and then dissolved in DEPC-treated water. A NanoDrop 2000/2000c spectrophotometer (Thermo Scientific, Waltham, USA) was used to measure the concentration and purity of RNA. Samples having A260/A280 ratios between 1.8 and 2.0 were used for further analysis. The PrimeScript RT Reagent Kit (Takara, Kusatsu, Japan) was used to create cDNA. Quantitative real-time PCR was then performed on a Thermo Fisher QuantStudio 5 system using SYBR Green chemistry (Takara, Kusatsu, Japan), with 16S rRNA as the endogenous control. Gene expression levels were calculated using the $2^{-\Delta\Delta Ct}$ method.[42] All primer sequences used in this study are listed in Table 1.

Membrane Permeability Assays

The integrity of the bacterial membrane following FCZ_Au NPs treatment was assessed by evaluating membrane permeability. This was done using the fluorescent probes N-phenyl-1-naphthylamine (NPN) and propidium iodide (PI), following established protocols. NPN fluoresces enter the damaged outer membrane of Gram-negative bacteria, while PI enters cells with compromised cytoplasmic membranes, providing a comprehensive assessment of membrane damage.[43,44] After adjusting the bacterial suspensions to an OD_{600} of 0.3–0.4, they were treated with four groups (each at 0.5 × MIC of FCZ_Au NPs). After washing and centrifugation at 3500 rpm, the bacterial pellets were harvested and resuspended in a solution containing 30 μM NPN and 50 μg/mL PI. The suspension was then incubated at 37°C for 30 min, after which the fluorescence was measured using a microplate reader at excitation/emission wavelengths of 350/420 nm for NPN and 535/615 nm for PI.

In vivo Antibacterial Activity

We selected mice for the in vivo experiments. Healthy male CD-1 (ICR) mice aged 28 to 34 days were purchased from Vital River in Zhejiang, China, with body weights ranging between 24 and 30 g. All mouse experiments were approved by the Ethics Committee of the First Affiliated Hospital of Wenzhou Medical University (Approval No. SYXK 2021–0017) and conducted in full compliance with the Wenzhou Laboratory Animal Welfare and Ethics Guidelines. We established mouse intraperitoneal infection model to evaluate the effect of FCZ_Au NPs on survival rate, following a previously described method.[45] The mice were randomly divided into four groups, with ten mice in each group. Each receiving an intraperitoneal injection of 200 μL FK8712 suspension (1.5×10^8 CFU/mL). Two hours post-infection, the four groups received intraperitoneal injections of PBS, FCZ (5 mg/kg), Au NPs (5 mg/kg), or FCZ_Au NPs (5 mg/kg),

Table 1 Oligonucleotides Used in This Study

Primer	Sequence (5'-3')
16S-F	ACTCCTACGGGAGGCAGCAGT
16S-R	TATTACCGCGGCTGCTGGC
soxS-F	GATGTTCCGTACCGTCATG
soxS-R	GAAGGTTTGCTGCGAGAC

https://doi.org/10.2147/IDR.S588073

respectively. Survival status was monitored and recorded every 12 h for 96 h after treatment. Additionally, a bacterial load assessment was performed using the same infection model. At the 24-hour endpoint following treatment, mice were anesthetized with 3% isoflurane and sacrificed by cervical dislocation. Peritoneal lavage fluid was then aseptically collected from each mouse, and the bacterial burden was determined via performing standard colony-forming unit (CFU) counts.

Biocompatibility Analysis

We evaluated the hemolytic activity of FCZ_Au NPs according to a previously described method.[46] Briefly, a 5% red blood cell (RBC) solution (from healthy mouse blood) was incubated with varying doses of FCZ_Au NPs in order to assess hemolytic activity. The negative control was PBS and positive control was 0.1% Triton X-100. Following centrifugation, the supernatant was carefully collected to avoid disturbing the pellet, then measured at a wavelength of 540 nm. The hemolysis rate was calculated [Hemolysis percentage $=\left(\text{absorbance}_{\text{experimental group}}-\text{absorbance}_{\text{negative group}}\right)/\left(\text{absorbance}_{\text{positive group}}-\text{absorbance}_{\text{negative group}}\right)\times 100\%$], and a value below 5% was considered safe.[47,48]

Additionally, the cytotoxicity of FCZ_Au NPs was assessed.[49] RAW264.7 cells were seeded in 96-well plates and subsequently exposed to a range of FCZ_Au NP concentrations. Following the treatment incubation, 10 μL of CCK-8 reagent (Solarbio, China) was added. The plates were subsequently incubated for 2 h in the dark. Finally, the absorbance was measured at 450 nm using a microplate reader for the quantification of cell viability.

Statistical Analysis

All quantitative data presented in the graphs are expressed as the mean ± standard deviation (SD). Statistical analyses and graph generation were performed using GraphPad Prism 10. Survival data were analyzed by the Kaplan-Meier method. For comparisons across more than two groups, one-way analysis of variance (ANOVA) was employed, followed by Tukey's post-hoc test for multiple comparisons. The following symbols were used to denote statistical significance throughout the study: * $p < 0.05$; ** $p < 0.01$; *** $p < 0.001$; **** $p < 0.0001$; ns, $p > 0.05$.

Results

Characterization of Synthesized FCZ_Au NPs

Currently, the one-pot synthesis method represents a highly convenient and rapid approach for nanoparticle preparation.[50] UV-Vis spectroscopy analysis of the synthesized FCZ_Au NPs revealed a characteristic peak at 540 nm (Figure 2A), which is typical for spherical gold nanoparticles. This finding was corroborated by DLS measurements, which indicated an average hydrodynamic diameter of 38.97 nm and a polydispersity index (PDI) of 0.295 (Figure 2B). Together, these data collectively confirm the successful synthesis of relatively small and monodisperse nanoparticles. The average zeta potential of FCZ_Au NPs was measured to be −22.52 mV (Figure 2C), suggesting a negatively charged surface and good colloidal stability. Additionally, TEM images revealed that FCZ_Au NPs had a high degree of dispersion and an irregular shape (Figure 2D). FTIR analysis further verified the effective synthesis of FCZ_Au NPs by seeing distinctive changes in the O–H (3463 cm^{-1}), C=O (1733 cm^{-1}), and C–O (1092 cm^{-1}) absorption peaks. The fluconazole benzene and triazole rings' C-H stretching was identified as the cause of a faint peak at 681 cm^{-1}. These results indicate that fluconazole was successfully loaded onto the surface of the gold nanoparticles via interactions such as hydrogen bonding, forming a FCZ_Au NPs complex (Figure 2E).

In vitro Antibacterial Activity of FCZ_Au NPs

By using broth microdilution, the MICs of compounds against the eight CRKP strains were ascertained (Table 2). While FCZ and Au NPs alone showed poor activity (MICs of 256 and 512 μg/mL, respectively), FCZ_Au NPs exhibited significantly enhanced efficacy, with MICs ranging from 4 to 16 μg/mL.

The dynamic antibacterial effects of FCZ_Au NPs in vitro were monitored via bacterial growth curves over a 24-h period (Figure 3). A key observation was the complete suppression of bacterial growth throughout the entire incubation period in the FCZ_Au NPs group. This stood in stark contrast to the robust and significant growth observed in the other groups. Together, these data collectively validate the potent and superior anti-CRKP efficacy of FCZ_Au NPs.

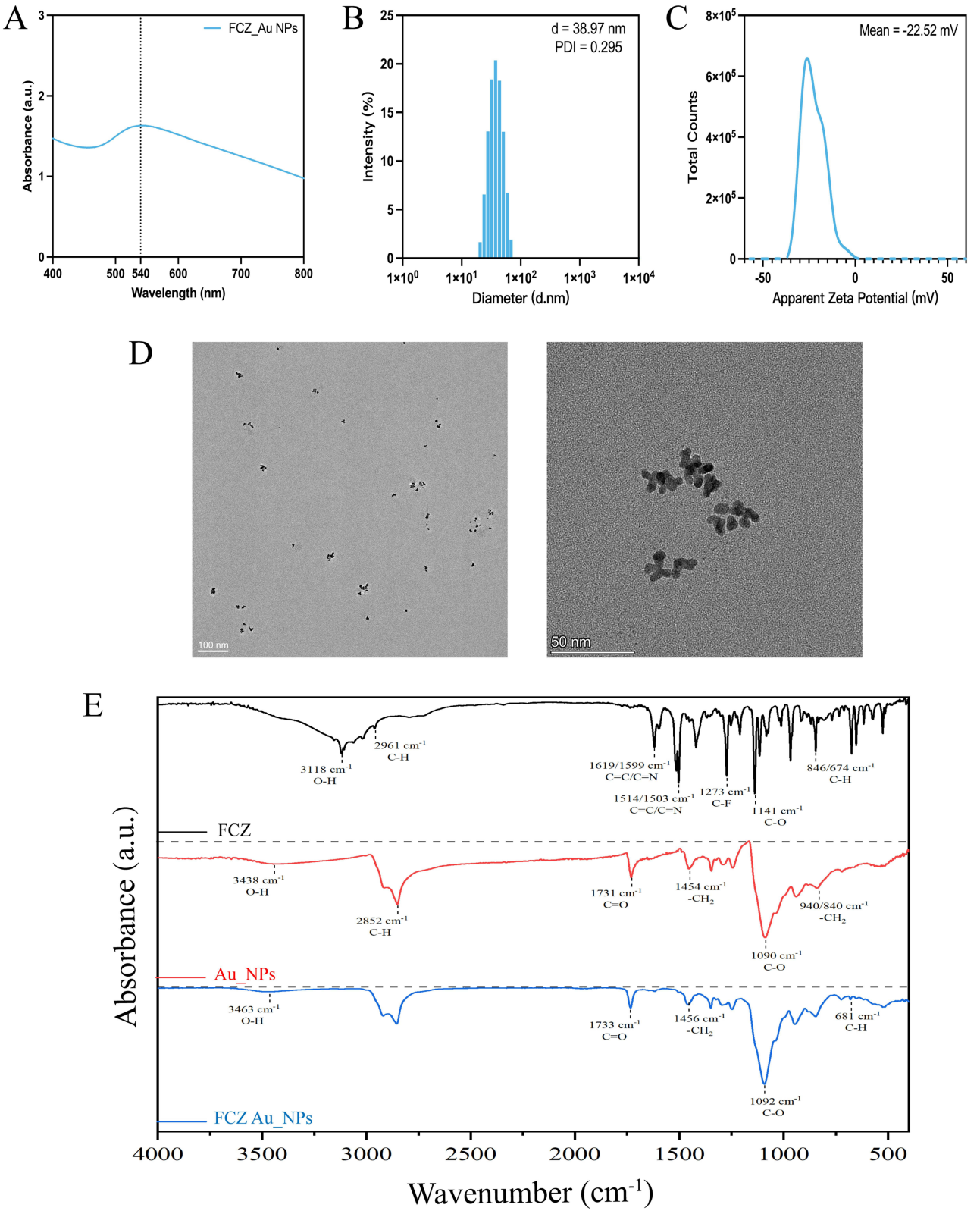

Figure 2 Synthesis and characterization of FCZ_Au NPs. (**A**) Ultraviolet absorption spectrum of FCZ_Au NP. (**B**) Particle size and dispersity of FCZ_Au NPs. (**C**) Zeta potential of FCZ_Au NPs. (**D**) TEM images of FCZ_Au NPs (**E**) FTIR spectra of FCZ_Au NPs, FCZ, and Au NPs.

https://doi.org/10.2147/IDR.S588073

Table 2 Antimicrobial Susceptibility of the FCZ, Au NPs, and FCZ_Au NPs Against Carbapenem-Resistant *K. pneumoniae* Strains

Species	Strains	Antibiotics[a]			Non-Antibiotics[c]		
		Breakpoints (S-R)[b] MIC (mg/L)			MIC (mg/L)		
		IPM 1–4	MEM 1–4	ETP 0.5–2	FCZ	Au NPs	FCZ_AuNPs
K. pneumoniae	FK8160	64	256	≥512	≥256	≥512	8
	FK8165	64	256	≥512	≥256	≥512	8
	FK8191	64	256	≥512	≥256	≥512	8
	FK8224	8	32	256	≥256	≥512	16
	FK8712	8	16	64	≥256	≥512	4
	FK8777	8	32	128	≥256	≥512	8
	FK8812	8	16	64	≥256	≥512	8
	FK8839	8	16	128	≥256	≥512	8

Notes: [a]IPM, imipenem; MEM, meropenem; ETP, ertapenem. [b]S-R represents the susceptible (S) breakpoint to resistant (R) breakpoint, according to CLSI supplement M100 (35th edition) and EUCAST. [c]FCZ, fluconazole.

Anti-Biofilm Activity of FCZ_Au NPs

Biofilms maintain bacterial structural integrity, facilitate adhesion to surfaces, and enhance antibiotic resistance by protecting embedded cells from antimicrobial agents.[51,52] This highlights the importance of eradicating bacterial biofilms. We assessed the anti-biofilm efficacy of FCZ_Au NPs via the crystal violet staining method. The results demonstrated that FCZ_Au NPs effectively inhibited both biofilm formation (Figure 4A) and pre-existing mature biofilms (Figure 4B).

Investigation of the Antibacterial Mechanisms of FCZ_Au NPs

By inducing severe oxidative stress, excessive ROS leading to bacterial cell death.[53] We measured intracellular ROS levels following drug treatment. The FCZ_Au NPs-treated group exhibited a marked increase in ROS levels relative to all other groups, implicating oxidative stress as a key antibacterial mechanism (Figure 5). To molecularly substantiate this

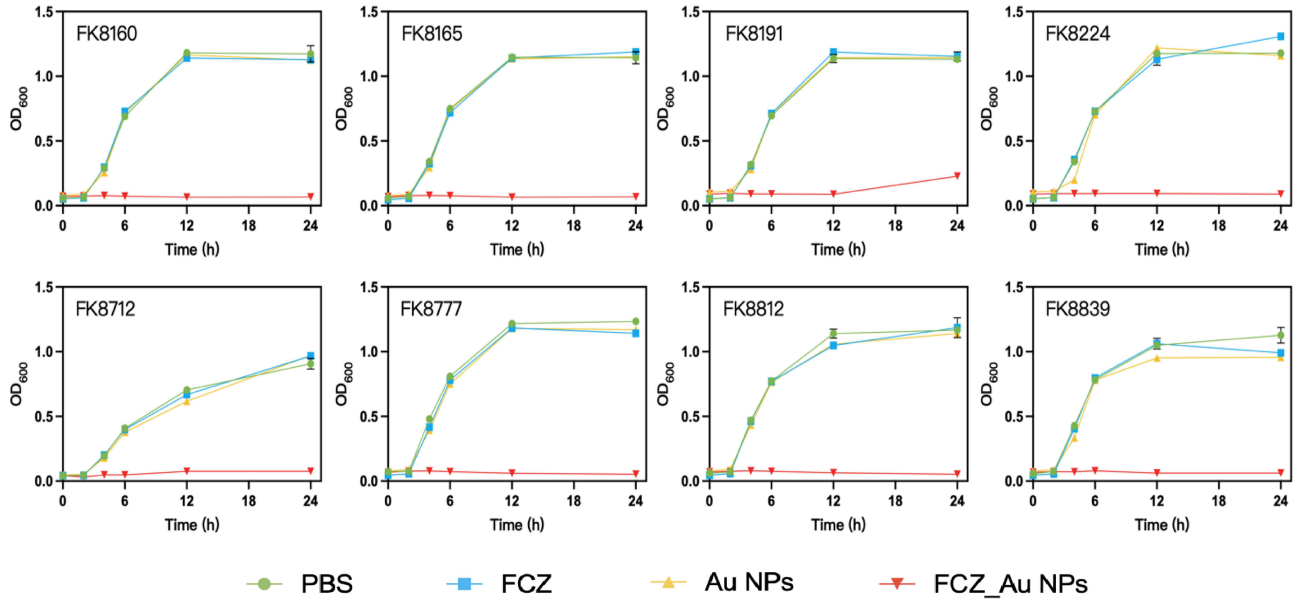

Figure 3 The growth curve results of eight CRKP strains after treatment in each group.

https://doi.org/10.2147/IDR.S588073

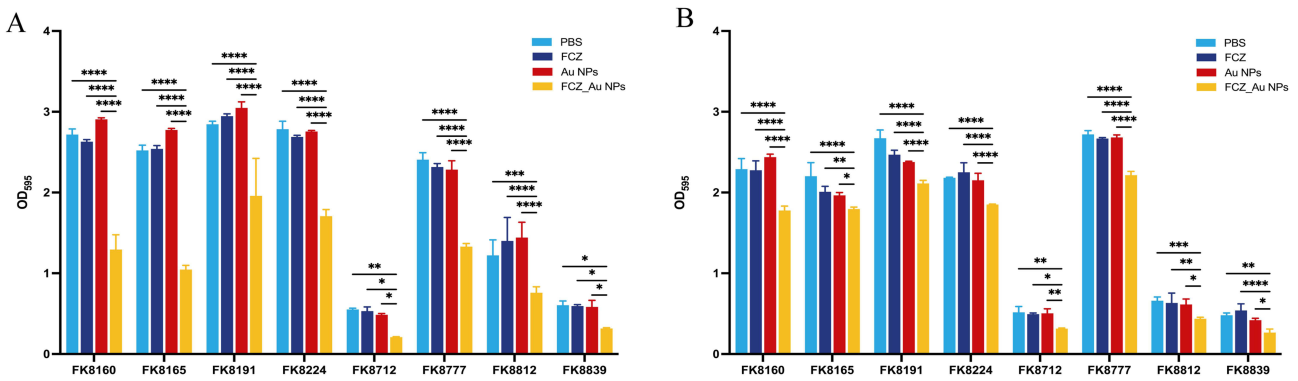

Figure 4 Anti-biofilm activity of FCZ_Au NPs. (**A**) Inhibition of biofilm formation of eight bacteria strains after treatment in each group. (**B**) Removal of mature biofilm of eight bacteria strains after treatment in each group. **P* < 0.05; ***P* < 0.01; ****P* < 0.001; *****P* < 0.0001.

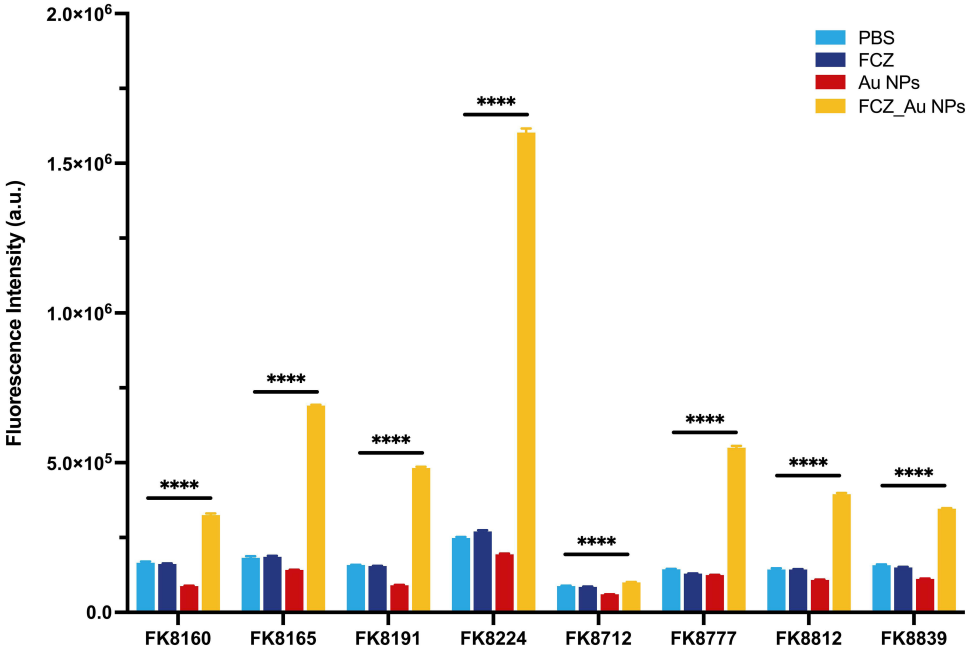

Figure 5 The level of ROS in eight bacteria strains after treatment in each group. *****P* < 0.0001.

finding, we quantified the expression of the *soxS*. This gene serves as a key transcriptional regulator activated during oxidative stress and is rapidly upregulated when bacteria encounter adverse environments, making it a sensitive indicator of intracellular oxidative damage.[54] Relative to other groups, *soxS* expression was significantly upregulated in the FCZ_AuNPs-treated group (Figure 6). This indicates that the bacteria encountered unfavorable conditions after FCZ_AuNPs treatment, which triggered a compensatory stress response.

The bacterial cell membrane is a critical barrier against antimicrobial agents, and its damage increases permeability, thereby enhancing bactericidal effects.[55,56] In this study, membrane permeability was assessed using the fluorescent probes NPN and PI for outer and inner membrane integrity, respectively. The results demonstrated that treatment with FCZ_Au NPs at 0.5 × MIC increased outer membrane permeability (Figure 7A) as well as inner membrane permeability (Figure 7B) across all eight tested strains.

https://doi.org/10.2147/IDR.S588073

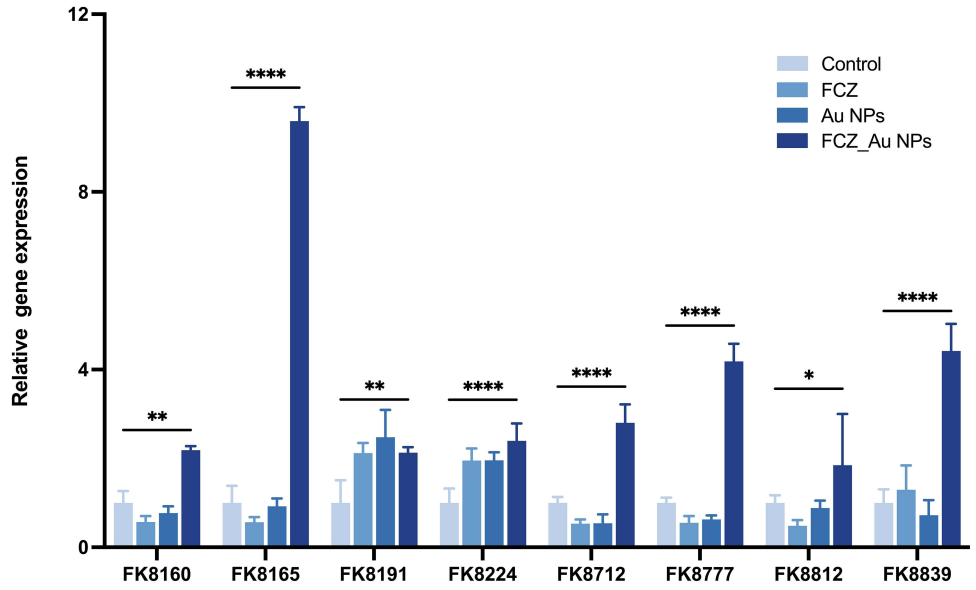

Figure 6 The expression level of soxS in eight bacteria strains after treatment in each group. *P < 0.05; **P < 0.01; ****P < 0.0001.

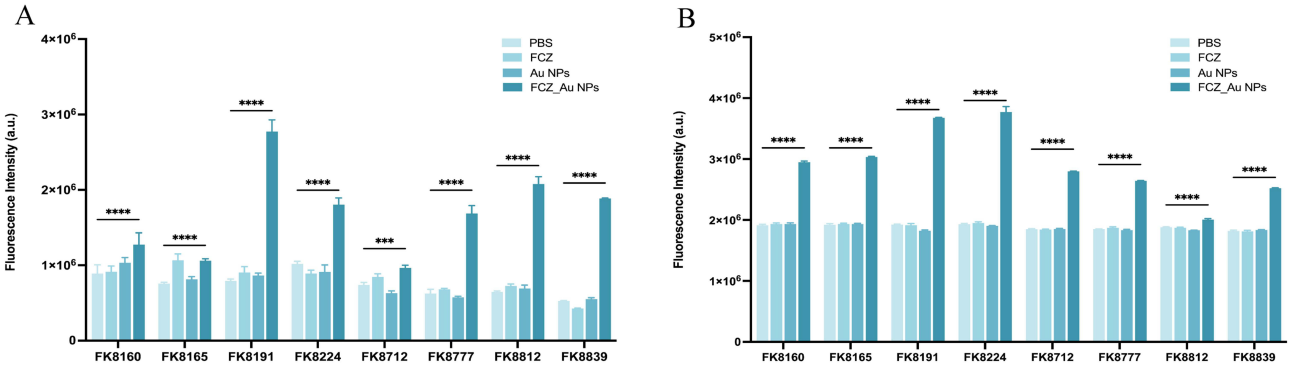

Figure 7 Antibacterial mechanisms of FCZ_Au NPs. (**A**) Assessment of bacterial outer membrane permeability using the NPN assay. (**B**) Assessment of bacterial inner membrane permeability using the PI assay. ***P < 0.001; ****P < 0.0001.

Evaluation of the in vivo Antibacterial Activity of FCZ_Au NPs

To establish the abdominal infection model, mice were intraperitoneally inoculated with a standardized bacterial suspension. Treatments were administered 2 h post-inoculation, using PBS as a control, and survival rates were monitored at 12-hour intervals. The results demonstrated a significant survival advantage in the FCZ_Au NPs-treated group over the other three groups at 96 h (Figure 8A). Furthermore, bacterial colony counts from peritoneal fluid revealed a highly significant reduction in bacterial counts in mice treated with FCZ_Au NPs (Figure 8B). Collectively, these findings demonstrate that FCZ_Au NPs possess a dual advantage: significant in vitro antibacterial activity against CRKP, coupled with promising in vivo therapeutic outcomes, as evidenced by improved survival rates and decreased bacterial burden in the murine intraperitoneal infection model. This underscores their potential as a viable candidate for further development against challenging CRKP infections.

Safety Assessment of FCZ_Au NPs

The safety of the drug concentrations used in this study was assessed through a series of experiments. The RBC hemolysis assay showed that at 32 μg/mL and below, the hemolysis rate induced by FCZ_Au NPs was less than 5%, indicating that FCZ_Au NPs exhibited no significant hemolytic activity at antibacterial effective concentrations (Figure 9A). Meanwhile, results from the cytotoxicity assay demonstrated that FCZ_Au NPs exhibited no significant

 https://doi.org/10.2147/IDR.S588073

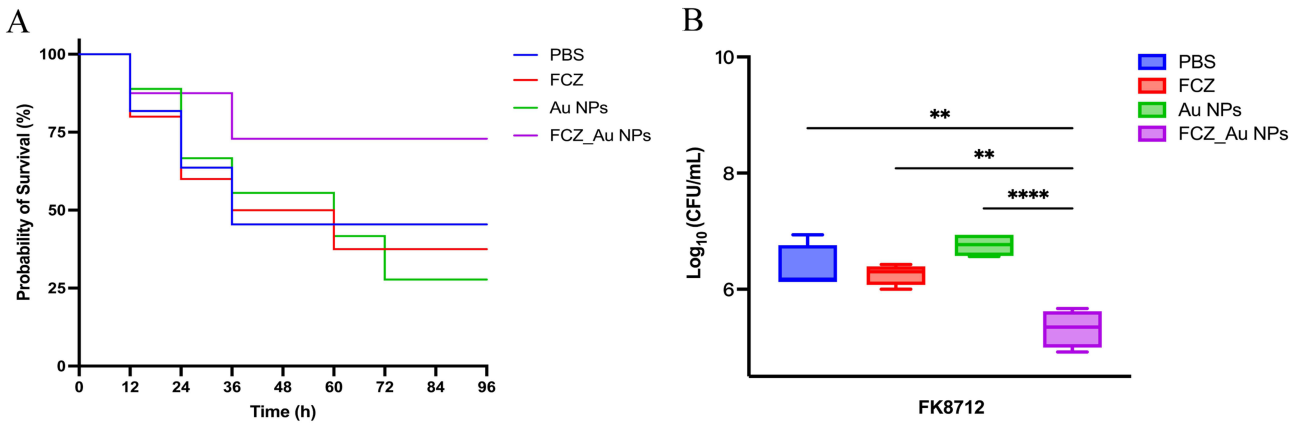

Figure 8 In vivo antibacterial activity of FCZ_Au NPs. (**A**) 96-hour survival rates of mice in different treatment groups after FK8712 infection. (**B**) Bacterial load in the peritoneal cavity of mice from different treatment groups after FK8712 infection. $^{**}P < 0.01$; $^{****}P < 0.0001$.

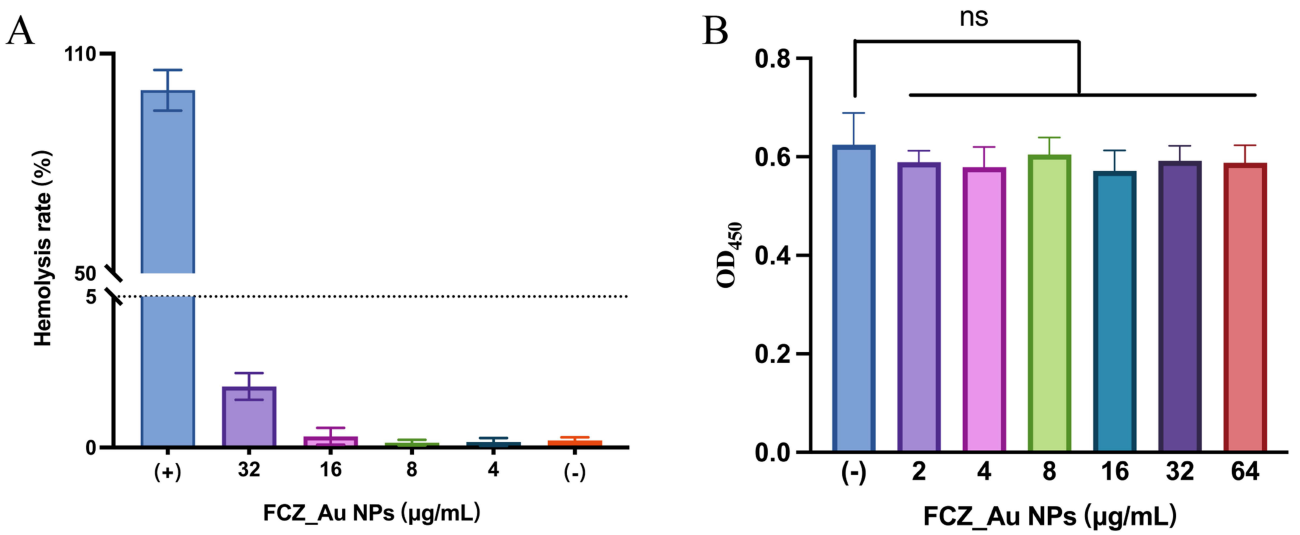

Figure 9 The Biocompatibility of FCZ_Au NPs. (**A**) Hemolytic rate of red blood cells after FCZ_Au NPs-treatment with different concentrations. (**B**) Cytotoxicity of FCZ_Au NPs at different concentrations. ns, $P > 0.05$.

toxicity to RAW264.7 cells even at 64 μg/mL (Figure 9B). In summary, these preliminary experiments showed that FCZ_Au NPs exhibit a favorable safety profile at the tested concentrations.

Discussion

Antimicrobial resistance (AMR) poses a worldwide concern driven by the dissemination of bacteria and resistance genes across human, animal, and environmental reservoirs.[57,58] Infections caused by carbapenem-resistant Enterobacteriaceae (CRE), especially CRKP, lead a formidable challenge in global infectious disease control due to limited therapeutic options.[59–61] Given this challenge, new treatment modalities are urgently needed. Au NPs have garnered significant research interest, Au NPs have tunable optical characteristics and ease of surface functionalization, which underpin their diverse applications across biomedical and other fields. Previous studies have shown that Au NPs possess inherent antibacterial potential and can enhance the efficacy of antimicrobial photodynamic therapy.[62–64]

FCZ_Au NPs was successfully synthesized by conjugating the surface of Au NPs with the therapeutically utilized antifungal drug fluconazole. The nanoparticles had a PDI of 0.29 and an average hydrodynamic size of 38.97 nm. This narrow size distribution suggests high dispersion stability, which is favorable for cellular uptake. The antibacterial activity of FCZ_Au NPs

https://doi.org/10.2147/IDR.S588073

was confirmed by both in vivo and in vitro tests, underscoring their promising potential to combat challenging infections. The biosafety assessments, including hemolysis and cytotoxicity assays, confirmed the preliminary safety of FCZ_Au NPs at tested concentrations. However, future efforts should focus on optimizing the formulation of FCZ-Au NPs to enhance its stability and targeting efficiency. Additionally, comparative studies with existing nanotherapeutic strategies, such as silver nanoparticles or other drug-functionalized platforms, will be essential to establish the relative advantages and limitations of this approach. Addressing these aspects in subsequent research will be critical for advancing FCZ-Au NPs toward clinical translation.

The bacterial cell membrane serves as the first barrier against external threats. Consequently, disruption of this barrier through altered permeability can induce cell lysis and death. Our results revealed that treatment with FCZ_AuNPs increased the permeability of membranes. This process may originate from two aspects: the interactions of nanoparticle surface functional groups with the bacterial outer membrane, along with the specific binding of FCZ to its components. Together, these effects may lead to membrane structural disruption, creating conditions for subsequent intracellular actions. Further studies revealed that FCZ_Au NPs induce ROS accumulation, confirming that oxidative stress represents a major mechanism underlying the antibacterial action. ROS production compromises cellular antioxidant defenses and induces mechanical damage to cell membranes.[65,66] As highly reactive oxidizing molecules, ROS can cause cell death by damaging bacterial DNA, proteins, and lipid membranes. Moreover, membrane disruption may exacerbate intracellular ROS accumulation: increased membrane permeability promotes the cellular uptake of FCZ_Au NPs, where their interaction with components such as respiratory chain proteins directly triggers ROS generation. However, this still requires further experimental investigation and validation. The *soxS*, a central regulator of the oxidative stress response, is upregulated under ROS-induced stress to mitigate and repair oxidative damage, once the damage exceeds the bacterial regulatory capacity, it can still cause irreversible harm to the cells.[67] In this study, FCZ_AuNPs treatment significantly elevated ROS levels, triggering the upregulation of *soxS* as an adaptive response to oxidative stress. However, when the damage exceeded the bacterial regulatory capacity, it resulted in irreversible bacterial death. Consequently, the upregulation of *soxS* also serves as corroborating evidence that ROS accumulation is one of the antibacterial mechanisms. The specific underlying mechanisms require further investigation.

In this study, we successfully constructed FCZ_Au NPs and systematically evaluated their activity against CRKP. Through a series of experiments, we confirmed the significant bactericidal effect of this nanoplatform and preliminarily revealed that it may damage bacteria by inducing oxidative stress. However, this study has certain limitations that need to be addressed in future work. First, regarding the antibacterial mechanism, the current exploration remains relatively superficial and has not yet reached the molecular level. Specifically, the interaction between FCZ_Au NPs and specific bacterial outer membrane proteins has not been clarified. Moreover, although we observed an increase in ROS levels, the decisive intracellular targets attacked by ROS that lead to bacterial death remain to be identified. Elucidating these issues requires screening differentially expressed proteins using proteomics and validating them by constructing specific gene knockout strains, thereby fully elucidating the antibacterial mechanisms at the molecular level. Second, in terms of in vivo efficacy evaluation, the current infection model is relatively singular. The pharmacodynamic data in this study are primarily based on an abdominal infection model. However, clinical epidemiological data indicate that CRKP infections are most common in the lungs of patients receiving mechanical ventilation and in the urinary tract environment with indwelling catheters. Given that different infection microenvironments may affect the activity of nanoparticles, future research should establish pneumonia and urinary tract infection models to more accurately assess their actual efficacy in primary clinical lesions. Finally, concerning clinical translation, the distribution, degradation, and excretion pathways of FCZ_Au NPs in vivo remain to be clarified. Although preliminary observations suggest a certain level of biosafety, data on their long-term toxicity and comprehensive pharmacokinetic characteristics are still lacking. Addressing these issues is crucial for advancing their clinical translation.

Conclusion

This study developed a novel nanoconjugate by decorating gold nanoparticles with fluconazole, which exhibited potent antimicrobial and anti-biofilm effects against CRKP. The underlying mechanism was attributed to a multi-target action, including simultaneous damage to the bacterial membranes and induction of intracellular ROS production. This nanoconstruct also showed excellent biocompatibility in preliminary safety assessments, thus representing a promising nanoplatform worthy of further preclinical investigation.

Data Sharing Statement

The data that support the findings of this study are available from the corresponding author upon reasonable request.

Ethics Approval

All mouse experiments were approved by the Ethics Committee of the First Affiliated Hospital of Wenzhou Medical University (Approval No. SYXK 2021-0017) and conducted in full compliance with the Wenzhou Laboratory Animal Welfare and Ethics Guidelines.

Acknowledgments

This study was funded by the Health Department of Zhejiang Province of the People's Republic of China (Grant no. 2022KY202), the Consortium for Infection and Innovation (CII) of The First Affiliated Hospital of Wenzhou Medical University (Grant no. 2025WMU-X001). We sincerely appreciate to the collaborative atmosphere and academic assistance within our laboratory community.

Author Contributions

All authors made a significant contribution to the work reported, whether that is in the conception, study design, execution, acquisition of data, analysis and interpretation, or in all these areas; took part in drafting, revising or critically reviewing the article; gave final approval of the version to be published; have agreed on the journal to which the article has been submitted; and agree to be accountable for all aspects of the work.

Funding

This study was funded by the Health Department of Zhejiang Province of the People's Republic of China (Grant no. 2022KY202), the Consortium for Infection and Innovation (CII) of The First Affiliated Hospital of Wenzhou Medical University (Grant no. 2025WMU-X001).

Disclosure

The authors report no conflicts of interest in this work.

References

1. Rotman E, McClure S, Glazier J, et al. Rapid design of bacteriophage cocktails to suppress the burden and virulence of gut-resident carbapenem-resistant *Klebsiella pneumoniae*. *Cell Host Microbe*. 2024;32(11). doi:10.1016/j.chom.2024.09.004
2. Li L, Gao X, Li M, et al. Relationship between biofilm formation and antibiotic resistance of *Klebsiella pneumoniae* and updates on antibiofilm therapeutic strategies. *Front Cell Infect Microbiol*. 2024;14:1324895.
3. Bray AS, Broberg CA, Hudson AW, et al. *Klebsiella pneumoniae* employs a type VI secretion system to overcome microbiota-mediated colonization resistance. *Nat Commun*. 2025;16(1):940. doi:10.1038/s41467-025-56309-8
4. Sá-Pessoa J, Calderón-González R, Lee A, Bengoechea JA. *Klebsiella pneumoniae* emerging anti-immunology paradigms: from stealth to evasion. *Trends Microbiol*. 2025;33(5):533–545. doi:10.1016/j.tim.2025.01.003
5. Wyres KL, Lam MMC, Holt KE. Population genomics of *Klebsiella pneumoniae*. *Nat Rev Microbiol*. 2020;18(6):344–359. doi:10.1038/s41579-019-0315-1
6. Arato V, Raso MM, Gasperini G, Berlanda Scorza F, Micoli F. Prophylaxis and treatment against *Klebsiella pneumoniae*: current insights on this emerging anti-microbial resistant global threat. *Int J Mol Sci*. 2021;22(8). doi:10.3390/ijms22084042
7. Rodriguez de Evgrafov M, Gumpert H, Munck C, Thomsen TT, Sommer MOA. Collateral resistance and sensitivity modulate evolution of high-level resistance to drug combination treatment in Staphylococcus aureus. *Mol Biol Evol*. 2015;32(5):1175–1185. doi:10.1093/molbev/msv006
8. He S, Yang Z, Li X, et al. Boosting stability and therapeutic potential of proteolysis-resistant antimicrobial peptides by end-tagging β-naphthylalanine. *Acta Biomater*. 2023;164:175–194.
9. Chen H, Liu H, Gong Y, et al. A Klebsiella-phage cocktail to broaden the host range and delay bacteriophage resistance both in vitro and in vivo. *NPJ Biofilms Microbiomes*. 2024;10(1):127. doi:10.1038/s41522-024-00603-8
10. Shi S, Xu M, Zhao Y, et al. Tigecycline-rifampicin restrains resistance development in carbapenem-resistant *Klebsiella pneumoniae*. *ACS Infect Dis*. 2023;9(10):1858–1866. doi:10.1021/acsinfecdis.3c00186
11. Jeon E, Kim MK, Park Y. Efficacy of the bee-venom antimicrobial peptide Osmin against sensitive and carbapenem-resistant *Klebsiella pneumoniae* strains. *Int J Antimicrob Agents*. 2023;63(2):107054. doi:10.1016/j.ijantimicag.2023.107054
12. Li L, Zeng Y, Tian M, et al. The antimicrobial peptide Cec4 has therapeutic potential against clinical carbapenem-resistant *Klebsiella pneumoniae*. *Microbiol Spectr*. 2025;13(7):e0273824. doi:10.1128/spectrum.02738-24

13. Zhao M, Li H, Gan D, Wang M, Deng H, Yang QE. Antibacterial effect of phage cocktails and phage-antibiotic synergy against pathogenic *Klebsiella pneumoniae*. *mSystems*. 2024;9(9):e0060724. doi:10.1128/msystems.00607-24
14. Farokhzad OC, Langer R. Impact of nanotechnology on drug delivery. *ACS Nano*. 2009;3(1):16–20. doi:10.1021/nn900002m
15. Turkmen Koc SN, Rezaei Benam S, Aral IP, Shahbazi R, Ulubayram K. Gold nanoparticles-mediated photothermal and photodynamic therapies for cancer. *Int J Pharm*. 2024;655:124057.
16. Maťátková O, Michailidu J, Miškovská A, Kolouchová I, Masák J, Čejková A. Antimicrobial properties and applications of metal nanoparticles biosynthesized by green methods. *Biotechnol Adv*. 2022;58:107905.
17. Ali M. What function of nanoparticles is the primary factor for their hyper-toxicity? *Adv Colloid Interface Sci*. 2023;314:102881.
18. Ahmad S, Ahmad S, Ali S, Esa M, Khan A, Yan H. Recent advancements and unexplored biomedical applications of green synthesized ag and au nanoparticles: a review. *Int J Nanomed*. 2024;19:3187–3215.
19. Singh J, Dutta T, Kim K-H, Rawat M, Samddar P, Kumar P. 'Green' synthesis of metals and their oxide nanoparticles: applications for environmental remediation. *J Nanobiotechnology*. 2018;16(1):84. doi:10.1186/s12951-018-0408-4
20. Jiang Z, Li L, Huang H, He W, Ming W. Progress in laser ablation and biological synthesis processes: "Top-Down" and "Bottom-Up" approaches for the green synthesis of Au/Ag nanoparticles. *Int J Mol Sci*. 2022;23(23). doi:10.3390/ijms232314658
21. Hernández-Díaz JA, Garza-García JJ, Zamudio-Ojeda A, León-Morales JM, López-Velázquez JC, García-Morales S. Plant-mediated synthesis of nanoparticles and their antimicrobial activity against phytopathogens. *J Sci Food Agric*. 2020;101(4):1270–1287. doi:10.1002/jsfa.10767
22. Qamar SUR. Nanocomposites: potential therapeutic agents for the diagnosis and treatment of infectious diseases and cancer. *Colloid Interface Sci. Commun*. 2021;43:100463.
23. Qamar SUR, Ahmad JN. Nanoparticles: mechanism of biosynthesis using plant extracts, bacteria, fungi, and their applications. *J Mol Liq*. 2021;334:116040.
24. Ali S, Chen X, Ajmal Shah M, et al. The avenue of fruit wastes to worth for synthesis of silver and gold nanoparticles and their antimicrobial application against foodborne pathogens: a review. *Food Chem*. 2021;359:129912.
25. Singh P, Pandit S, Beshay M, et al. Anti-biofilm effects of gold and silver nanoparticles synthesized by the *Rhodiola rosea* rhizome extracts. *Artif Cells Nanomed Biotechnol*. 2018;46(sup3):S886–S899. doi:10.1080/21691401.2018.1518909
26. Cai R, Cheng Q, Zhao J, et al. Sericin-assisted green synthesis of gold nanoparticles as broad-spectrum antimicrobial and biofilm-disrupting agents for therapy of bacterial infection. *Int J Nanomed*. 2025;20:3559–3574.
27. Makabenta JMV, Nabawy A, Li C-H, Schmidt-Malan S, Patel R, Rotello VM. Nanomaterial-based therapeutics for antibiotic-resistant bacterial infections. *Nat Rev Microbiol*. 2020;19(1):23–36. doi:10.1038/s41579-020-0420-1
28. Zhu P, Zhou T, Chen H, et al. Novel triazoles with potent and broad-spectrum antifungal activity in vitro and in vivo. *J Med Chem*. 2023;66 (11):7497–7515. doi:10.1021/acs.jmedchem.3c00266
29. Cousin L, Berre ML, Launay-Vacher V, Izzedine H, Deray G. Dosing guidelines for fluconazole in patients with renal failure. *Nephrol Dial Transplant*. 2003;18(11):2227–2231. doi:10.1093/ndt/gfg363
30. Lu H, Shrivastava M, Whiteway M, Jiang Y. *Candida albicans* targets that potentially synergize with fluconazole. *Crit Rev Microbiol*. 2021;47 (3):323–337. doi:10.1080/1040841X.2021.1884641
31. Behtash A, Nafisi S, Maibach HI. New generation of fluconazole: a review on existing researches and technologies. *Curr Drug Deliv*. 2017;14(1). doi:10.2174/1567201813666160502125620
32. Pandey R, Crutchfield N, Garren MRS, et al. Combating concomitant bacterial and fungal infections via codelivery of nitric oxide and fluconazole. *ACS Appl Mater Interfaces*. 2025;17(16):23613–23626. doi:10.1021/acsami.5c00174
33. Anwar A, Siddiqui R, Raza Shah M, Ahmed Khan N. Gold nanoparticles conjugation enhances antiacanthamoebic properties of nystatin, fluconazole and amphotericin B. *J Microbiol Biotechnol*. 2019;29(1):171–177. doi:10.4014/jmb.1805.05028
34. Rattanata N, Klaynongsruang S, Leelayuwat C, et al. Gallic acid conjugated with gold nanoparticles: antibacterial activity and mechanism of action on foodborne pathogens. *Int J Nanomed*. 2016;11:3347–3356.
35. Momeni S, Ghorbani-Vaghei R. A facile one-pot synthesis of tetrahydrobenzo[b]pyrans and 2-amino-4H-chromenes under green conditions. *RSC Adv*. 2024;14(30):21608–21622. doi:10.1039/D4RA04239E
36. Zhang W, Jiang W. Antioxidant and antibacterial chitosan film with tea polyphenols-mediated green synthesis silver nanoparticle via a novel one-pot method. *Int J Biol Macromol*. 2019;155:1252–1261.
37. Belanger CR, Hancock REW. Testing physiologically relevant conditions in minimal inhibitory concentration assays. *Nat Protoc*. 2021;16 (8):3761–3774. doi:10.1038/s41596-021-00572-8
38. Yu M, Hou Y, Cheng M, et al. Antibacterial activity of squaric amide derivative SA2 against methicillin-resistant Staphylococcus aureus. *Antibiotics*. 2022;11(11). doi:10.3390/antibiotics11111497
39. Giordani B, Naldi M, Croatti V, et al. Exopolysaccharides from vaginal lactobacilli modulate microbial biofilms. *Microb Cell Fact*. 2023;22(1):45. doi:10.1186/s12934-023-02053-x
40. Ding T, Wang S, Zhang X, et al. Kidney protection effects of dihydroquercetin on diabetic nephropathy through suppressing ROS and NLRP3 inflammasome. *Phytomedicine*. 2018;41:45–53.
41. Veilleux C, Roy M-È, Zgheib A, Desjarlais M, Annabi B. Evidence for a JAK2/STAT3 proinflammatory and vasculogenic mimicry interrelated molecular signature in adipocyte-derived mesenchymal stromal/stem cells. *Cell Commun Signal*. 2025;23(1):291. doi:10.1186/s12964-025-02298-6
42. Li S, Sun D, Chen S, et al. UCP2-SIRT3 signaling relieved hyperglycemia-induced oxidative stress and senescence in diabetic retinopathy. *Invest Ophthalmol Vis Sci*. 2024;65(1):14. doi:10.1167/iovs.65.1.14
43. Soh SM, Jang H, Mitchell RJ. Loss of the lipopolysaccharide (LPS) inner core increases the electrocompetence of *Escherichia coli*. *Appl Microbiol Biotechnol*. 2020;104(17):7427–7435. doi:10.1007/s00253-020-10779-6
44. Yang X, Zhao S, Deng Y, et al. Antibacterial activity and mechanisms of α-terpineol against foodborne pathogenic bacteria. *Appl Microbiol Biotechnol*. 2023;107(21):6641–6653. doi:10.1007/s00253-023-12737-4
45. Wang N, Sheng Q, Zhu H, et al. Enhancing the effectiveness of Polymyxin E with a fisetin nanoemulsion against a colistin-resistant Salmonella typhimurium infection. *Phytomedicine*. 2024;130:155768.
46. Liu H, Huang Z, Chen H, et al. A potential strategy against clinical carbapenem-resistant Enterobacteriaceae: antimicrobial activity study of sweetener-decorated gold nanoparticles in vitro and in vivo. *J Nanobiotechnology*. 2023;21(1):409. doi:10.1186/s12951-023-02149-x

47. Tong X, Shi Z, Xu L, et al. Degradation behavior, cytotoxicity, hemolysis, and antibacterial properties of electro-deposited Zn-Cu metal foams as potential biodegradable bone implants. *Acta Biomater*. 2019;102:481–492.
48. Pan J, Zhang J, Hu P, et al. Daidzein-decorated gold nanoparticles as a novel antimicrobial strategy against carbapenem-resistant Enterobacteriaceae. *Int J Nanomed*. 2025;20:7811–7827.
49. Yu C, Qiu G, Liu X, et al. Anti-inflammatory effect and mechanism of stytontriterpene D on RAW264.7 cells and zebrafish. *Front Pharmacol*. 2025;161:559022.
50. Tian Y, Qi J, Zhang W, Cai Q, Jiang X. Facile, one-pot synthesis, and antibacterial activity of mesoporous silica nanoparticles decorated with well-dispersed silver nanoparticles. *ACS Appl Mater Interfaces*. 2014;6(15):12038–12045. doi:10.1021/am5026424
51. Guo Z, Liu M, Zhang D. Potential of phage depolymerase for the treatment of bacterial biofilms. *Virulence*. 2023;14(1):2273567. doi:10.1080/21505594.2023.2273567
52. Jeong G-J, Khan F, Tabassum N, Cho K-J, Kim Y-M. Bacterial extracellular vesicles: modulation of biofilm and virulence properties. *Acta Biomater*. 2024;178:13–23.
53. Ruhland BR, Reniere ML. Sense and sensor ability: redox-responsive regulators in Listeria monocytogenes. *Curr Opin Microbiol*. 2018;47:20–25.
54. Anes J, Dever K, Eshwar A, et al. Analysis of the oxidative stress regulon identifies soxs as a genetic target for resistance reversal in multidrug-resistant *Klebsiella pneumoniae*. *mBio*. 2021;12(3):e0086721. doi:10.1128/mBio.00867-21
55. Je J-Y, Kim S-K. Chitosan derivatives killed bacteria by disrupting the outer and inner membrane. *J Agric Food Chem*. 2006;54(18):6629–6633. doi:10.1021/jf061310p
56. Xie R, Taylor RJ, Kahne D. Outer membrane translocon communicates with inner membrane ATPase to stop lipopolysaccharide transport. *J Am Chem Soc*. 2018;140(40):12691–12694. doi:10.1021/jacs.8b07656
57. Larsson DGJ, Flach C-F. Antibiotic resistance in the environment. *Nat Rev Microbiol*. 2021;20(5):257–269. doi:10.1038/s41579-021-00649-x
58. Abbas A, Barkhouse A, Hackenberger D, Wright GD. Antibiotic resistance: a key microbial survival mechanism that threatens public health. *Cell Host Microbe*. 2024;32(6):837–851. doi:10.1016/j.chom.2024.05.015
59. Ma J, Song X, Li M, et al. Global spread of carbapenem-resistant Enterobacteriaceae: epidemiological features, resistance mechanisms, detection and therapy. *Microbiol Res*. 2022;266:127249.
60. Di Pilato V, Pollini S, Miriagou V, Rossolini GM, D'Andrea MM. Carbapenem-resistant *Klebsiella pneumoniae*: the role of plasmids in emergence, dissemination, and evolution of a major clinical challenge. *Expert Rev Anti Infect Ther*. 2024;22(1–3):25–43. doi:10.1080/14787210.2024.2305854
61. El-Mahallawy HA, El Swify M, Abdul Hak A, Zafer MM. Increasing trends of colistin resistance in patients at high-risk of carbapenem-resistant Enterobacteriaceae. *Ann Med*. 2022;54(1):1–9. doi:10.1080/07853890.2022.2129775
62. Mandhata CP, Bishoyi AK, Sahoo CR, et al. Investigation of in vitro antimicrobial, antioxidant and antiproliferative activities of Nostoc calcicola biosynthesized gold nanoparticles. *Bioprocess Biosyst Eng*. 2023;46(9):1341–1350. doi:10.1007/s00449-023-02905-1
63. Wang C, Singh P, Kim YJ, et al. Characterization and antimicrobial application of biosynthesized gold and silver nanoparticles by using Microbacterium resistens. *Artif Cells Nanomed Biotechnol*. 2015;44(7):1714–1721. doi:10.3109/21691401.2015.1089253
64. Maliszewska I, Wanarska E, Thompson AC, Samuel IDW, Matczyszyn K. Biogenic gold nanoparticles decrease methylene blue photobleaching and enhance antimicrobial photodynamic therapy. *Molecules*. 2021;26(3). doi:10.3390/molecules26030623
65. Basavegowda N, Baek K-H. Multimetallic nanoparticles as alternative antimicrobial agents: challenges and perspectives. *Molecules*. 2021;26(4). doi:10.3390/molecules26040912
66. Wahab S, Salman A, Khan Z, Khan S, Krishnaraj C, Yun S-I. Metallic nanoparticles: a promising arsenal against antimicrobial resistance-unraveling mechanisms and enhancing medication efficacy. *Int J Mol Sci*. 2023;24(19). doi:10.3390/ijms241914897
67. Wang P, Zhang H, Liu Y, et al. SoxS is a positive regulator of key pathogenesis genes and promotes intracellular replication and virulence of Salmonella Typhimurium. *Microb Pathog*. 2019;139:103925.